Narrow-band single-photon emission in the near infrared for quantum key distribution

E Wu and Vincent Jacques

Laboratoire de Photonique Quantique et Moléculaire, UMR CNRS 8537, Ecole Normale Supérieure de Cachan, France

Heping Zeng

Key Laboratory of Optical and Magnetic Resonance Spectroscopy, East China Normal Univerity, Shanghai 200062, P.R. China

Philippe Grangier

Laboratoire Charles Fabry de l'Institut d'Optique, UMR CNRS 8501, France

François Treussart and Jean-François Roch

Laboratoire de Photonique Quantique et Moléculaire, UMR CNRS 8537, Ecole Normale Supérieure de Cachan, France

francois.treussart@physique.ens-cachan.fr

Abstract: We present a detailed study of photophysical properties of single color centers in natural diamond samples emitting in the near infrared under optical excitation. Photoluminescence of these single emitters has several striking features, including narrow-band (FWHM 2 nm) fully polarized emission around 780 nm, a short excited-state lifetime of about 2 ns, and perfect photostability at room temperature under our excitation conditions. Development of a triggered single-photon source relying on this single color center is discussed for application to quantum key distribution.

OCIS codes: (270.5290) Photon Statistics; (160.4760) Optical properties; (170.1790) Confocal microscopy

References and links

1. P. Grangier, B. Sanders, and J. Vučković editors, "Focus on Single Photons on Demand," New J. Phys. **6** (2004).
2. C.H. Bennett and G. Brassard, "Quantum cryptography: public key distribution and coin tossing," Proceedings of the IEEE International Conference on Computers, Systems & Signal Processing (Bangalore, India), 175-179 (1984).
3. N. Gisin, G. Ribordy, W. Tittel, and H. Zbinden, "Quantum cryptography," Rev. Mod. Phys. **74**, 145-195 (2002).
4. C. Gerry and P. Knight, *Introductory quantum optics* (Cambridge University Press, Cambridge, 2005).
5. N. Lütkenhaus, "Estimates for practical quantum cryptography," Phys. Rev. A **59**, 3301-3320 (1999).
6. A. Beveratos, R. Brouri, T. Gacoin, A. Villing, J.-P. Poizat, and P. Grangier, "Single photon quantum cryptography," Phys. Rev. Lett. **89**, 187901 (2002).
7. R. Alléaume, F. Treussart, G. Messin, Y. Dumeige, J.-F. Roch, A. Beveratos, R. Brouri-Tualle, J.-P. Poizat, and P. Grangier, "Experimental open-air quantum key distribution with a single-photon source," New J. Phys. **6**, 92 (2004).
8. W.-Y. Hwang, "Quantum key distribution with high loss: toward global secure communication," Phys. Rev. Lett. **91**, 057901 (2003).
9. H.-K. Lo, X. Ma, and K. Chen, "Decoy state quantum key distribution," Phys. Rev. Lett. **94**, 230504, 2005.
10. P. Grangier, G. Roger, and A. Aspect, "Experimental evidence for a photon anticorrelation effect on a beam splitter: a new light on single-photon interferences," Europhys. Lett. **1**, 173-179 (1986).

#9540 - $15.00 USD Received 15 November 2005; revised 20 January 2006; accepted 23 January 2006

11. C.K. Hong and L. Mandel, "Experimental realization of a localized one-photon state," Phys. Rev. Lett. **56**, 58-60 (1986).
12. S. Fasel, O. Alibart, S. Tanzilli, P. Baldi, A. Beveratos, N. Gisin, and H. Zbinden, "High-quality asynchronous heralded single-photon source at telecom wavelength," New J. Phys. **6**, 163 (2004).
13. O. Alibart, D.B. Ostrowsky, P. Baldi, and S. Tanzilli, "High performance guided-wave asynchroneous heralded single-photon source," Opt. Lett. **30**, 1539-1541 (2005).
14. R. Alléaume, J.-F. Roch, D. Subacius, A. Zavriyev, and A. Trifonov, "Fiber-optics quantum cryptography with single photons," AIP Conference Proceedings **734**, 287-290 (2004).
15. R. Brouri, A. Beveratos, J.-Ph. Poizat, and P. Grangier, "Single-photon generation by pulsed excitation of a single dipole," Phys. Rev. A **62**, 063817-063823 (2000).
16. F. De Martini, G. Di Giuseppe, and M. Marrocco, "Single-mode generation of quantum photon states by excited single molecules in a microcavity trap," Phys. Rev. Lett. **76**, 900-903 (1996).
17. A. Beveratos, S. Kühn, R. Brouri, T. Gacoin, J.-P. Poizat, and P. Grangier, "Room temperature stable single photon source," Eur. Phys. J. D **18**, 191 (2002).
18. A. M. Zaitsev, *Optical properties of diamond, a data handbook* (Springer, Berlin , 2000).
19. T. Gaebel, I. Popa, A. Gruber, M. Domhan, F. Jelezko, and J. Wrachtrup, "Stable single-photon source in the near infrared," New J. Phys. **6**, 98 (2004).
20. J. Rabeau, Y. Chin, S. Prawer, F. Jelezko, T. Gaebel, and J. Wrachtrup, "Fabrication of single nickel-nitrogen defects in diamond by chemical vapor deposition," Appl. Phys. Lett. **86**, 131926 (2005).
21. V. Nadolinny, A. Yelisseyev, J. Baker, M. Newton, D. Twitchen, S. Lawson, O. Yuryeva, and B. Feigelson, "A study of ^{13}C hyperfine structure in the EPR of nickel-nitrogen-containing centres in diamond and correlation with optical properties," J. Phys.: Condens. Matter. **11**, 7357-7376 (1999).
22. Their are four covalent bonds between nitrogen atoms and the nickel defect, but the electrons shared in each bond come from one atom species only, which is the specificity of coordination-type bond.
23. R. Brouri, A. Beveratos, J.-P. Poizat, and P. Grangier, "Photon antibunching in the fluorescence of individual colored centers in diamond," Opt. Lett. **25**, 1294-1296 (2000).
24. J. Isberg, J. Hammersberg, E. Johansson, T. Wikström, D. Twitchen, A. Whitehead, S. Coe, and G. Scarsbrook, "High carrier mobility in single-crystal plasma-deposited diamond," Science **297**, 1670-1672 (2002).
25. A. Beveratos, R. Brouri, T. Gacoin, J.-P. Poizat, and P. Grangier, "Nonclassical radiation from diamond nanocrystal," Phys. Rev. A **64**, 061802 (2001).
26. S. Reynaud, "La fluorescence de résonance: étude par la méthode de l'atome habillé," Ann. Phys. Fr. **8**, 315-370 (1983).
27. A. Yelisseyev, S. Lawson, I. Sildos, A. Osvet, V. Nadolinny, B. Feigelson, J.M. Baker, M. Newton, and O. Yuryeva, "Effect of HPHT annealing on the photoluminescence of synthetic diamonds grown in the Fe–Ni–C system," Diamond Relat. Mater. **12**, 2147-2168 (2003).
28. S. Kitson, P. Jonsson, J. Rarity, and P. Tapster, "Intensity fluctuation spectroscopy of small number of dye molecules in a microcavity," Phys. Rev. A **58**, 620-627 (1998).
29. F. Treussart, A. Clouqueur, C. Grossman, and J.-F. Roch, "Photon antibunching in the fluorescence of a single dye molecule embedded in a thin polymer film," Opt. Lett. **26**, 1504-1506 (2001).

1. Introduction

Significant recent efforts have been focused on development of new and reliable single-photon sources, due to an increasing number of applications for these sources in quantum optics, in quantum cryptography and for the realization of optical quantum gates [1]. For instance, basic proofs of quantum key distribution (QKD) security rely on encoding information on single quantum objects, namely single-photon light pulses [2]. Most practical QKD systems use weak coherent pulses as a quasi single-photon sources, which greatly simplifies experimental implementation [3]. However, faint laser pulses with mean photon number smaller than unity can still contain more than one photon due to the associated Poissonian photon number statistics [4]. Increasing attenuation on the quantum channel to lower the probability of multiphoton pulses is a practical solution, but it also reduces the secret key creation rate. Moreover, due to dark count detector noise, the secret bit rate in the most commonly used QKD Bennett and Brassard BB84 protocol [2] can drop to zero at a certain distance because of losses on the transmission channel [5]. Security improvement in long-distance QKD can indeed be achieved with single-photon sources as already demonstrated experimentally [6, 7] or new protocols, such as the one relying on decoy states [8, 9].

#9540 - $15.00 USD Received 15 November 2005; revised 20 January 2006; accepted 23 January 2006

Single photons can be conditionally prepared using a pair emission process such as atomic cascade [10] or spontaneous parametric down-conversion [11]. One photon of the emitted pair "triggers" field mode preparation for a second photon in a single-photon state. With this scheme, single photons at telecom wavelengths can be prepared efficiently using bulk $\chi^{(2)}$ nonlinear crystals [12] or guided-wave nonlinear devices [13]. These systems have been experimentally confirmed as promising for long-distance QKD in optical fiber [14]. Unfortunately, emission time remains random in this type of single-photon generation. In a quantum cryptography-based communication system, it is highly desirable to deal with single photons triggered by an external clock.

Clock-triggered single photons can be efficiently produced by pulsed excitation of the emitting dipole [15], which undergoes a complete cycle of excitation, emission, and reexcitation before emitting the next photon. Since first proposal by De Martini *et al.* [16] a variety of single-photon source implementation schemes have been realized, many relying on fluorescence of isolated single emitters including atoms, molecules, color centers, and semiconductor quantum dots (see Ref. [1] for a recent review).

A reliable triggered single-photon source based on photoluminescence of single Nitrogen-Vacancy (NV) color centers in diamond nanocrystal was recently realized with pulsed optical excitation at room temperature [17]. This turn-key single-photon source was then implemented in QKD experiments using polarization-encoded single-photon sequences in the BB84 protocol [6, 7]. As theoretically expected [5], single-photon light pulses show measurable advantages over faint laser pulses for quantum channel security and key creation rate in the high attenuation regime.

The wide variety of photostable color centers in diamond [18] offers opportunity to optimize single-photon properties for practical QKD applications. For instance, polarized single-photon emission, together with nanosecond-range excited state lifetime and nanometer spectral bandwidth, are desired. Recently, the Nickel-related defect NE8 was observed at the single emitter level, both in natural diamond [19] and CVD diamond film [20]. In the NE8 center, the Nickel atom is located at equal distance of two carbon vacancies, and it is associated with four Nitrogen atoms in its first coordination shell [21, 22]. The NE8 color center is characterized by weak electron-phonon coupling and most of its photoluminescence is concentrated within the zero-phonon line (ZPL) of sharp emission (FWHM 1.5 nm) around 800 nm.

We report on our room-temperature observation of single diamond color centers, in the same wavelength range as the NE8 color center. Assumed to be Nickel-Nitrogen related impurities with perfect photostable luminescence at room temperature, we study their photoluminescent properties under optical excitation with a red cw diode laser. Both single-photon emission and metastable-state shelving are observed from photon time-correlation measurements with a Hanbury Brown and Twiss (HBT) setup. We show that these emitters meet the required properties for practical single-photon QKD as stated above. First, a narrow emission band is observed around 782 nm, which lies in both open-air and fiber-optics optical communication "window". Second, we infer an excited-state lifetime around 2 ns, compatible with narrow time-window analysis for reducing effects of photodetector dark count noise. Third, emitted light is linearly polarized, which is perfectly suitable for encoding polarization information on the emitted single photons.

2. Experimental set-up and results

We use a homemade scanning confocal microscope to select single defects in the sample (see Ref.[23] for a detailed description of the setup). The detection system includes a HBT setup with two silicon avalanche photodiodes (APDs) in the single-photon counting regime (SPCM, Perkin Elmer) on each side of a 50/50 non-polarizing beam splitter. It also integrates a spec-

#9540 - $15.00 USD Received 15 November 2005; revised 20 January 2006; accepted 23 January 2006

trograph with a cooled CCD array for recording spectrum. We first raster scan the sample ($2 \times 2 \times 0.32$ mm type IIa natural bulk diamond wafer from Element6, The Netherlands) to identify well-isolated photoluminescent emitters using a 687-nm diode laser for cw excitation. The laser beam is focused to a spot size of $\sim 1\mu$m FWHM about 4 μm below the sample surface. The microscope objective ($\times$100, NA$=$ 0.95) also collects emitted light. Figure 1(a) displays photoluminescence from a single Nickel-Nitrogen related defect in a 9×9 μm scan of the sample. The *z*-axis indicates the count rate for one APD of the HBT setup. From the scan in Fig. 1(a), the observed signal to background ratio of the photoluminescence is as large as 60 : 1. The weak remaining background light is ascribed to the photoluminescence of other color centers either of the same type but located in different planes than the imaged one, or to other less efficient but maybe more abundant photoluminescent defects. Using ultra-high purity CVD-grown diamond [24] or replacing the bulk sample by diamond nanoparticles [25] may reduce this background.

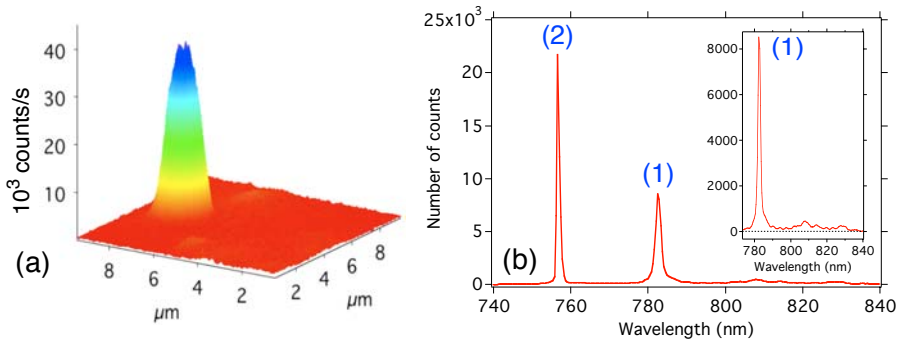

Fig. 1. (a) Fluorescence intensity raster scan of a natural diamond sample showing luminescence from an isolated color center. One APD output in the HBT setup gives maximum counting rate $\sim 4 \times 10^4$ counts/s. (b) Photoluminescence spectrum with 10 s integration for the single emitter observed in Fig. 1(a). This spectrum has been corrected for the quantum efficiency of the CCD, which varies from 53 to 85% in the 740–840 nm range considered. The narrow peak (1) at 782 nm ($\sim$ 2 nm FWHM) is the ZPL of the Nickel-Nitrogen related defect [19]. The sharp peak (2) at 756 nm is related to the one-phonon Raman scattering line of the diamond lattice with 1332 cm^{-1} frequency shift. *Inset*: ZPL, more clearly showing phonon wing intensity.

The HBT setup is used to investigate the fluorescence intensity correlation function. Thanks to narrow spectral emission, a bandpass filter placed before the HBT setup permits selection of defect photoluminescence while rejecting Raman scattering from the diamond crystalline lattice. Analysis of photodetection events gives a histogram of time delays between consecutively detected photons. This delay function is equivalent to the second-order intensity autocorrelation function for short time scales [26]. Antibunching evidence of single center emission appears as a dip in the recorded delay function around $t = 0$ (see Fig. 3(a)) as a consequence of finite time duration for the excitation-emission-reexcitation cycle of a single dipole [4].

At the same time, we record an emission spectrum for the single emitter. Figure 1(b) shows the spectrum for the emitter in Fig. 1(a). The narrow emission peak at 782 nm is tentatively ascribed to a Nickel-Nitrogen related impurity in diamond [18, 27]. From this spectrum, we infer that even at room temperature, about 70% of the total intensity is concentrated in the ZPL. This value is much higher than the $\sim$ 1% value for the Nitrogen-Vacancy color center.

We also investigated polarization properties of the single color center relative to absorption

#9540 - $15.00 USD Received 15 November 2005; revised 20 January 2006; accepted 23 January 2006

and emission. While rotating the linear polarization angle of the excitation laser, we monitored photoluminescence intensity and obtained oscillations with contrast of about 96%. This contrast value proves that the single color center behaves like a dipole for light absorption. We studied the emitted light polarization properties using a quarter-wave plate. The collected light is elliptically polarized with an aspect ratio of 0.25, indicating that the single defect also behaves like an emitting dipole. The linear polarized light becomes elliptical after propagation through a high numerical aperture objective and dichroic mirror, both known to modify polarization.

3. Photophysics of 782 nm emitting color centers

To investigate dynamical processes of photoluminescence, we model single color center response within the framework of a three-level system comprised of ground (1), excited (2), and metastable (3) levels as shown in Fig. 2.

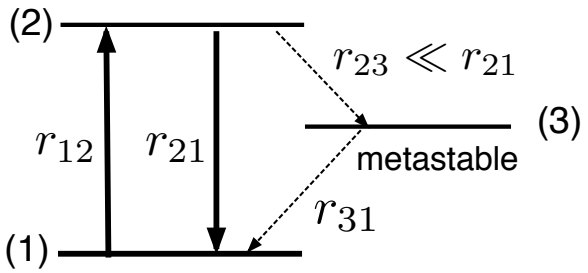

Fig. 2. Three-level system with corresponding decay and intersystem crossing rates.

The single color center is excited from its ground level. From its excited level, the center either returns to the ground level or non-radiatively decays to the metastable level, as indicated by photon bunching observed in the intensity correlation measurement. From this "dark" level, the system finally returns to the ground level by phosphorescence. These dynamics can be described by the following set of rate equations for populations $\{p_1, p_2, p_3\}$ of the three levels

$$\begin{cases} \dot{p_1} = & -r_{12}p_1 + r_{21}p_2 + r_{31}p_3 \\ \dot{p_2} = & r_{12}p_1 - (r_{21}+r_{23})p_2 \\ \dot{p_3} = & r_{23}p_2 - r_{31}p_3 \end{cases} \tag{1}$$

where r_{nm} (with $n,m = 1,2,3$) denotes the transition rate from level (n) to level (m). We assume that transition rates r_{23} and r_{31} to and from the metastable level, respectively, are small compared to the rate of decay r_{21} from excited to ground level. According to Ref. [28], from the normalized intensity correlation function

$$g^{(2)}(t) \equiv \frac{\langle I(0)I(t)\rangle}{\langle I(t)\rangle^2} \tag{2}$$

we infer the following analytical expression for $t \geq 0$

$$g^{(2)}(t) = p_2(0;t)/p_2(\infty) = 1-(1+a)e^{-\lambda_1 t} + ae^{-\lambda_2 t}, \tag{3}$$

$$\lambda_1 = r_{12} + r_{21}, \tag{4}$$

$$\lambda_2 = r_{31} + r_{23}r_{12}/(r_{12}+r_{21}), \tag{5}$$

$$a = r_{12}r_{23}/[r_{31}(r_{12}+r_{21})], \tag{6}$$

#9540 - $15.00 USD Received 15 November 2005; revised 20 January 2006; accepted 23 January 2006

where $p_2(\infty)$ is the steady-state population of the excited level (2) and $p_2(0;t)$ denotes the population of level (2) at time t, starting from level (1) at time $t=0$. Recalling that r_{23} and r_{31} are small compared to r_{21}, it follows that λ_1 is much larger than λ_2. The following two limiting expressions of Eq. 3 can then be found.
(i) On "short" time scales ($t \lesssim 20$ ns), the $g^{(2)}$ function exhibits photon antibunching:

$$g^{(2)}(t) \simeq 1-(1+a)e^{-\lambda_1 t}. \tag{7}$$

(ii) On "long" time scales ($t \gtrsim 20$ ns), antibunching associated with luminescence of the single emitter does not affect the $g^{(2)}$ function [29], such that:

$$g^{(2)}(t) \simeq 1+ae^{-\lambda_2 t}. \tag{8}$$

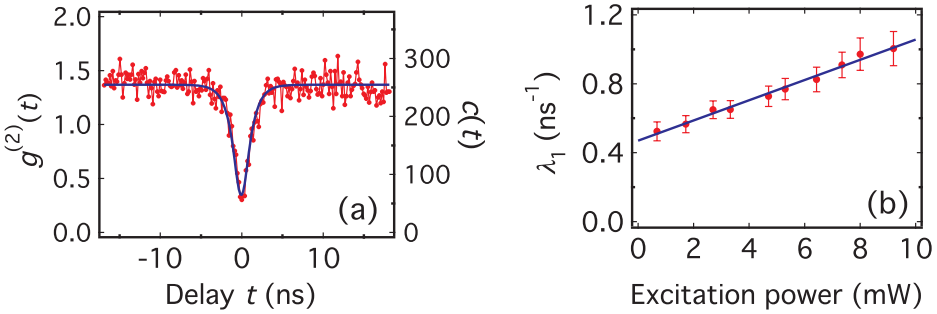

Fig. 3. (a) Photon coincidence number $c(t)$ (right scale) and normalized intensity correlation function $g^{(2)}(t)$ (left scale) recorded for a single emitter at short time scales ($|t| \lesssim 20$ ns). Excitation was carried out at 9 mW, the maximum available cw power. Integration duration was $T=590$ s, $R_1 \simeq 37000$ counts/s, $R_2 \simeq 48700$ counts/s, and time bin $w=0.17$ ns. Red dots represent experimental data, while the solid blue line is a convolution of Eq. (7) with the measured instrumental response function, with adjusted parameters a and λ_1. (b) Evolution of parameter λ_1 (red dots) as a function of excitation power with linear fitting (in blue), according to Eq. (4).

Normalization of the $g^{(2)}$ correlation function is inferred from the number of coincidences $c(t)$ recorded during an integration period T and for a time bin of width w

$$g^{(2)}(t) = \frac{c(t)}{R_1 R_2 T w}. \tag{9}$$

The factor R_1R_2T corresponds to the coincidence rate for an equivalent Poissonian photon number distribution associated with $R_{1,2}$ counts rates on each APD. This relation between $c(t)$ and $g^{(2)}(t)$ neglects any contribution from random background light emission, as assumed from the high signal-to-background ratio for the observed emitter in Fig. 1(a).

For a short time scale, the correlation function $g^{(2)}(t)$ and measured coincidences are represented in Fig. 3(a). It shows a distinct minimum at zero delay, with a residual non-zero value due to convolution with the instrumental response function (IRF) of the detection setup.

This function is independently measured to be a 1.2 ns FWHM Gaussian function, by correlation of Ti:Sa laser 150-fs laser pulses. Taking into account the IRF time, the measured intensity correlation function for our short time scale is fitted well by convolution of the IRF with the $g^{(2)}$ function given by Eq. (7).

#9540 - $15.00 USD Received 15 November 2005; revised 20 January 2006; accepted 23 January 2006

By fitting the $g^{(2)}$ function curve at short times for different excitation powers, we obtain the value of λ_1 as a function of excitation power (Fig. 3(b)). At zero excitation power, λ_1 is equal to the transition rate r_{21}, the inverted excited-level photon-emission lifetime. For the single emitter in Fig. 1(a), we obtain $r_{21} = 0.47$ ns^{-1} by extrapolating the linear fit to zero excitation power. Excited-level photon-emission lifetime is then calculated to be as short as 2 ns.

The absorption rate from the ground level is deduced from the dependence of λ_1 on excitation intensity, as given by $r_{12} = \sigma I/h\nu$ with absorption cross-section σ, excitation intensity I, and excitation frequency ν. From λ_1 at different excitation intensities, we obtain a power-independent absorbing cross-section $\sigma \simeq 1.7 \times 10^{-16}$ cm^2.

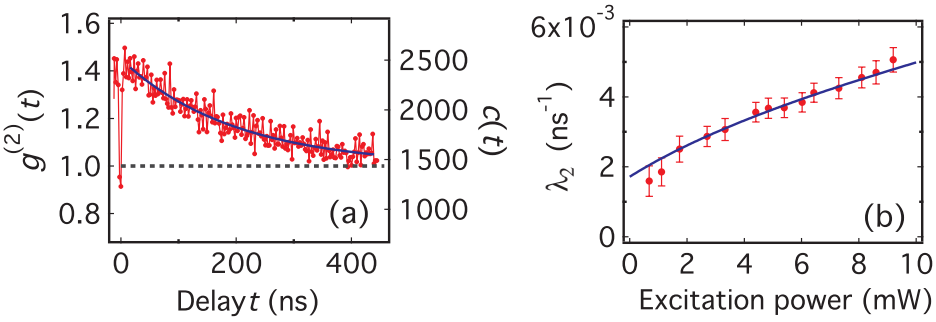

Fig. 4. (a) Number of photon coincidences $c(t)$ (right scale) and normalized intensity correlation function $g^{(2)}(t)$ (right scale) for a single emitter over a long time scale ($|t| \gtrsim$ 20 ns) with excitation power 9 mW, integration duration $T = 605$ s, $R_1 \simeq 38600$ counts/s, $R_2 \simeq 33400$ counts/s, and time bin $w = 2.3$ ns. Red dots represent experimental data, while the solid blue line fit is a convolution of Eq. (8) with measured instrumental response function. The dashed line indicates normalization corresponding to Poissonian photon-number statistics. The minimum value of $g^{(2)}$ at $t = 0$ appears higher than in Fig. 3(a) due to larger time bin for the histogram plot. (b) Evolution of parameter λ_2 (red dots) as a function of the excitation power, with fit (in blue) according to Eq. (5).

On long time scales, we observe $g^{(2)}(t) > 1$, corresponding to a bunching effect attributed to leakage into the "dark" metastable level (3) of the three-level model shown in Fig. 2. By fitting $g^{(2)}(t)$ without antibunching we obtain λ_2 as a function of excitation intensity (Fig. 4(b)). Intersystem crossing rates r_{23} and r_{31} are evaluated by fitting λ_2 using Eq. (5), together with r_{12} and r_{21} deduced from short time-scale measurements.

Treating r_{23} as a constant, we observe that the bunching effect depends on excitation power, indicating that 687 nm excitation light contributes to deshelving the metastable level. Indeed, our data are fitted well by assuming r_{31} dependence on excitation intensity (or, equivalently, on laser excitation power $P_{\rm ex}$) in the following manner $r_{31} = r_{31}^0(1+\beta P_{\rm ex})$, which gives $r_{23} = 2.75\ \mu$s^{-1}, $r_{31}^0 = 1.71\ \mu$s^{-1} and $\beta = 0.102$ mW^{-1}. This dependence of deshelving rate on excitation intensity is also observed for single molecules [29].

Using the parameters obtained above, the detected fluorescence rate is given by

$$R = \eta_{\rm det}\eta_{\rm Q}\,\frac{r_{21}}{(r_{21}/r_{12} + r_{23}/r_{31} + 1)}, \tag{10}$$

where R is the sum of count rates on the two APDs. Parameters $\eta_{\rm det}$ and η_Q represent the overall detection efficiency and the photoluminescence quantum yield, respectively. With decay rates obtained by fitting with intensity dependences λ_1 and λ_2, we obtain $\eta_{\rm det} \times \eta_{\rm Q} = 4.2 \times 10^{-4}$.

#9540 - $15.00 USD Received 15 November 2005; revised 20 January 2006; accepted 23 January 2006

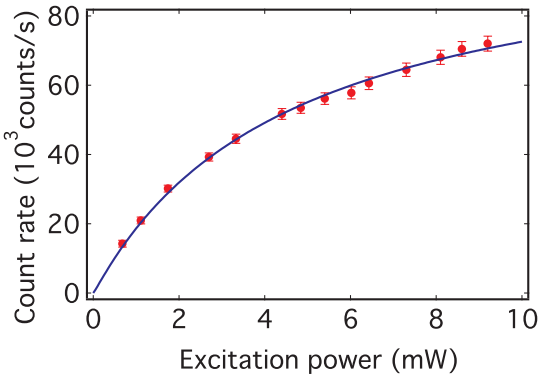

Fig. 5. Photoluminescence intensity measurement (circles with error bars) given by counting rate sum for both APDs, vs. excitation laser power. Fit given by Eq. (10) incorporates rate values r_{mn} calculated from measurements of λ_1 and λ_2. The fit is therefore achieved with a single free parameter, corresponding to the overall efficiency $\eta_{\mathrm{det}} \times \eta_{\mathrm{Q}}$.

In our experimental setup, η_{det} is limited by the collection efficiency of the microscope objective. Microscope parameters include: microscope objective with NA$=0.95$ working in air without immersion oil, $\eta_{\mathrm{col}} \simeq 2.6\%$, sphericity aberration $\eta_{\mathrm{ab}} \simeq 20\%$, objective transmittance $\eta_{\mathrm{trans}} \simeq 80\%$, optics (lens, dichroic mirror, filters) transmittance $\eta_{\mathrm{opt}} \simeq 35\%$, and silicon APDs quantum efficiency of $\eta_{\mathrm{APD}} \simeq 55\%$ in the near-infrared region. The estimated total detection efficiency is $\eta_{\mathrm{det}} = \eta_{\mathrm{col}} \times \eta_{\mathrm{ab}} \times \eta_{\mathrm{trans}} \times \eta_{\mathrm{opt}} \times \eta_{\mathrm{APD}} \simeq 8 \times 10^{-4}$. We finally roughly estimate the photoluminescence quantum yield to be $\eta_Q \simeq (52 \pm 20)\%$. While the quantum yield obviously needs a more precise evaluation, our estimate indicates that the measured short excited-state lifetime is associated with strong radiative oscillator strength, and not to efficient photoluminescence quenching through fast non-radiative decay processes which do not appear in the three level model.

4. Conclusion

We have studied photophysical properties of a color center, most likely of the Nickel-Nitrogen related type, with near-infrared emission at the single-emitter level. Assuming a three-level system, we have measured key photoluminescence parameters using the intensity correlation function on time scales both "short" and "long" compared to the emitter excited-level lifetime. This single diamond color center demonstrates favorable properties for applications in single-photon quantum information processing and quantum cryptography. A complementary study will determine optimal excitation wavelength to design a customized pulsed excitation laser for development of an efficient triggered single-photon source.

Acknowledgments

This work was supported by an "AC Nanosciences" grant from Ministère de la Recherche, by Institut Universitaire de France, and by Institut d'Alembert (ENS Cachan, IFR 121). This work was also partly funded by EADS/Corporate Research Center France (Suresnes, France) under contract n° 74166. E Wu is affiliated with "Key State Laboratory of Optical and Magnetic Resonance Spectroscopy," as part of the joint PhD program between Écoles Normales Supérieures and East China Normal University.

#9540 - $15.00 USD Received 15 November 2005; revised 20 January 2006; accepted 23 January 2006